

КРАТКИЕ СООБЩЕНИЯ

UDC 548.73:547.13

X-RAY STUDY OF THE THIRD POLYMORPHIC STRUCTURE OF  
μ-OXO-BIS[(OCTAETHYLPORPHINATO)IRON(III)]: [(OEPFe)<sub>2</sub>O]

M. Khorasani-Motlagh<sup>1</sup>, M. Noroozifar<sup>1</sup>, J. Saffari<sup>1</sup>, B.O. Patrick<sup>2</sup>

<sup>1</sup>Chemistry Department, University of Sistan & Baluchestan, Zahedan, Iran, e-mail: mkhorasani@chem.usb.ac.ir

<sup>2</sup>Chemistry Department, University of British Columbia, Vancouver, Canada

Received February, 24, 2011

Exposure of dichloromethane solution of [OEPFe<sup>III</sup>Cl], where OEP is the dianion of octaethylporphyrin, to dioxygen results in its transformation into the μ-oxo bridged compound [(OEPFe)<sub>2</sub>O]. The structure of [(OEPFe)<sub>2</sub>O] is determined by X-ray diffraction analysis. It contains binuclear centrosymmetric [(OEPFe)<sub>2</sub>O]. The Fe atom is five-coordinated to four N atoms of the porphyrin ring and to one bridging O atom. The compound is characterized by an average Fe—N bond length of 2.096 Å. The Fe—O bond distance is 1.7739(12) Å, the Fe—O—Fe bond angle is 180.0° and the two porphyrin rings are parallel. Crystal data: triclinic crystal system,  $a = 10.915(4)$ ,  $b = 12.951(4)$ ,  $c = 13.403(4)$  Å,  $\alpha = 118.06(1)^\circ$ ,  $\beta = 100.33(1)^\circ$ ,  $\gamma = 102.43^\circ$ ,  $P\bar{1}$  space group,  $V = 1144.5(1)$  Å<sup>3</sup>,  $Z = 1$ .

**К e y w o r d s:** heme, iron(III), octaethylporphyrin, oxo-dimer, crystal structure.

**Introduction.** The main thrust of the initial studies on metalloporphyrins arises from the biological functions of cytochrome P<sub>450</sub> enzymes that contain an iron porphyrin unit and are present in most organisms [1]. The iron porphyrin compounds play important roles as an oxygen transfer and storage agent in hemoglobin and myoglobin and as an electron carrier in the cytochrome. Metalloporphyrins have a square-planar geometry in which a metal ion is chelated by the four nitrogen atoms of a porphine ring with open coordination sites for axial ligation [2]. There have been several recent investigations of the effect of the relative orientations of planar axial ligands, and π-acceptor properties of axial ligands [3–5], on the structural and spectroscopic properties of Fe(III) porphyrinates [6]. The biological significance and rich chemistry of these compounds have promoted extensive research on model metalloporphyrins [2].

The end products of the irreversible bimolecular oxidation of Fe<sup>II</sup> species contain the Fe<sup>III</sup>—O—Fe<sup>III</sup> fragment. Given the facile formation of μ-oxodiiron(III) species, "it is not surprising that the Fe—O—Fe motif is incorporated into a variety of metalloproteins, including the oxygen-carrier hemerythrin, the hydrolase purple acid phosphatase, the oxidoreductases ribonucleotide reductase and methane monooxygenase, an iron-sulfur protein rubrerythrin, and iron-transport protein ferritin" [7].

We reported the isolation of new μ-oxodiiron(III) species with different counterions [8]. Here, we report a triclinic crystalline form of the μ-oxodiiron(III) complex [(OEPFe)<sub>2</sub>O] (1). Scheidt *et al.* reported two crystalline forms of [(OEPFe)<sub>2</sub>O]: one triclinic and one monoclinic [9]. We observed noticeable differences in the crystallographic parameters in comparison with those published before. We report the molecular structure of this μ-oxo bridged compound to compare these three crystalline forms.

**Experimental.** All solvents were dried by refluxing for several days over Na and benzophenone under Ar and distilled immediately before use. All reagents and solvents used in this study were obtained from Merck & Aldrich Chem. Co.

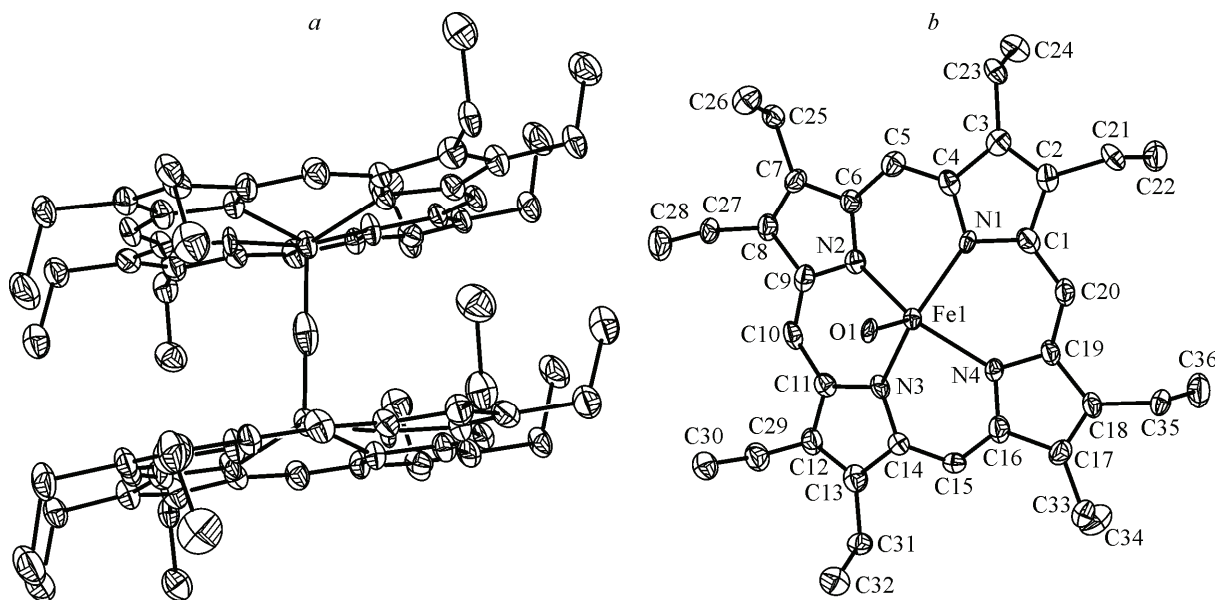


Fig. 1. (a) Perspective view diagram of the structure of  $[(\text{OEPFe})_2\text{O}]$  (1). The  $\text{Fe}—\text{O}—\text{Fe}$  is in the plane of the paper. Porphyrin hydrogen atoms are omitted for clarity. The atoms were drawn with 50 % probability ellipsoids.  
 (b) Drawing of a half-molecule of  $[(\text{OEPFe})_2\text{O}]$  (1) with atom labeling

UV-Vis spectra were recorded on an Analytic Jena SPE-CORD S100 spectrometer with a photodiode array detector. IR spectra were recorded as KBr disks on a Shimatzu IR instrument.

**Synthesis of  $[(\text{OEPFe}^{\text{III}})_2\text{O}]$ .** Oxygen was bubbled over 6 h through a solution of  $[\text{OEPFe}^{\text{III}}\text{Cl}]$  (20 mg) in dichloromethane (20 ml). The sample was evaporated to dryness under vacuum to give a dark red residue. The resulting red solid was recrystallized by dissolving it in a minimum volume of dichloromethane and slowly adding diethyl ether to precipitate the product. UV/vis absorption: 675, 350 nm. IR (KBr):  $\nu(\text{Fe}—\text{O}—\text{Fe}) = 875 \text{ cm}^{-1}$ . Crystal of  $[(\text{OEPFe}^{\text{III}})_2\text{O}]$  (1) was suitable for X-ray crystallography.

**Crystallography.** Crystallization of  $[(\text{OEPFe})_2\text{O}]$  (1) at room temperature by diffusion of ether into its saturated dichloromethane solution yielded good single crystals. Measurements were made on a Bruker X8 APEX diffractometer with graphite monochromated  $\text{MoK}_{\alpha}$  radiation ( $\lambda = 0.71073$ ). The data were collected at a temperature of  $-100 \pm 0.1 \text{ }^{\circ}\text{C}$  to a maximum  $2\theta$  value of  $45.6^{\circ}$ . Data were collected in a series of  $\varphi$  and  $\omega$  scans in  $0.50^{\circ}$  oscillations with 20.0-second exposures. The crystal-to-detector distance was 36.00 mm. The structure was solved by direct methods [10] and expanded using Fourier techniques [11]. The non-H-atoms were refined anisotropically. All hydrogen atoms were included in calculated positions but were not refined. The standard deviation of an observation of unit weight was 1.17. The material crystallizes with one half-molecule in the asymmetric unit, related to another half-molecule by inversion symmetry. The weighting scheme was based on counting statistics. The maximum and minimum peaks on the final difference Fourier map corresponded to  $1.83 \text{ e}^-/\text{\AA}^3$  and  $-0.66 \text{ e}^-/\text{\AA}^3$  respectively. Of the 13359 reflections that were collected, 4035 were unique ( $R_{\text{int}} = 0.059$ ); equivalent reflections were merged. The linear absorption coefficient  $\mu$  for  $\text{MoK}_{\alpha}$  radiation is  $5.22 \text{ cm}^{-1}$ . Data were corrected for absorption effects using the multi-scan technique (SADABS), with minimum and maximum transmission coefficients of 0.761 and 0.939 respectively.

A perspective view of  $[(\text{OEPFe})_2\text{O}]$  (1) with eclipsed configuration is depicted in Fig. 1. An overview of the molecular packing in the crystal structure of  $[(\text{OEPFe})_2\text{O}]$  (1) is shown in Fig. 2. Some details of the collection data are given in Table 1. Selected interaction distances and angles are given in Table 2. The complete crystallographic information file for the structure of the  $[(\text{OEPFe})_2\text{O}]$  (1) complex was deposited to CCDC, deposition number 765564, and is available free of charge at [www.ccdc.cam.ac.uk/conts/retrieving.html](http://www.ccdc.cam.ac.uk/conts/retrieving.html).

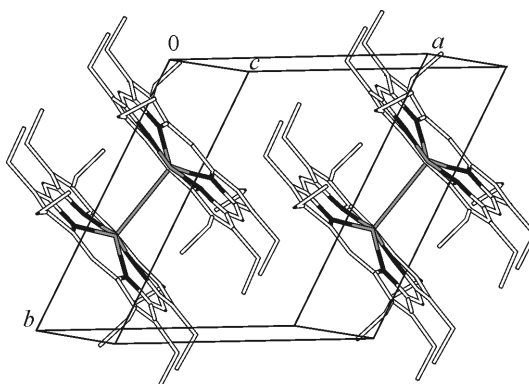


*Fig. 2.* Overview of molecular packing in the crystal structure of  $[(\text{OEPFe})_2\text{O}]$  (**1**)

**Results and discussion.** The results presented here show that the exposure of dichloromethane solution of  $[\text{OEPFe}^{\text{III}}\text{Cl}]$  to dioxygen results in its transformation into the  $\mu$ -oxo bridged compound  $[(\text{OEPFe})_2\text{O}]$ . Crystals of  $[(\text{OEPFe})_2\text{O}]$  (**1**) suitable for X-ray crystallography were prepared by the slow diffusion of diethyl ether into a dichloromethane solution of the complex.

Previously, Scheidt *et al.* reported two others crystalline forms of  $[(\text{OEPFe})_2\text{O}]$  [9]. Their X-ray quality crystals were prepared by dissolving the complex in dichloromethane and allowing hexanes (instead of diethyl ether for our prepared crystals) to diffuse into the solution. Crystallographic data for three crystalline forms of  $[(\text{OEPFe})_2\text{O}]$  are given in Table 3. As seen from Table 3, our molecular structure of  $[(\text{OEPFe})_2\text{O}]$  (**1**) is a triclinic crystalline form, and it has some differences in unit cell parameters with those of the reported crystalline forms of  $[(\text{OEPFe})_2\text{O}]$ .

The bridged oxygen atom sits on the inversion center and the average axial Fe—O bond length is 1.774 Å. The Fe—O distance of  $[(\text{OEPFe})_2\text{O}]$  (**1**) is slightly longer than 1.756 Å and 1.755 Å in two

T a b l e 1

*Crystallographic data for  $[(\text{OEPFe})_2\text{O}]$*

Chemical formula	$\text{C}_{72}\text{H}_{88}\text{N}_8\text{OFe}_2$	$T, \text{K}$	173.0(1)
Molecular weight	1193.20	$D, \text{g/cm}^3$	1.283
Crystal color	Black	$F(000)$	636.00
Crystal system	Triclinic	$\mu, \text{cm}^{-1}$	5.22
Space group	$P-1 (\#2)$	Tot. data colld	13359
$a, b, c, \text{\AA}$	10.915(4), 12.951(4), 13.403(4)	No. of unique data	4035 ( $R_{\text{int}} = 0.059$ )
$\alpha, \beta, \gamma, \text{deg.}$	118.06(1), 100.33(1), 102.43(1)	Final $R$ indices [ $I > 2\sigma(I)$ ]	$R_1 = 0.078; wR_2 = 0.225$
$V, \text{\AA}^3$	1144.5(1)	Final $R$ indices (for all data)	$R_1 = 0.120; wR_2 = 0.261$
$Z$	1	GOOF	1.17

$$R_1 = \sum ||F_0| - |F_c|| / \sum |F_0|, \quad wR_2 = \sqrt{\sum} (w(F_0^2 - F_c^2)^2) / \sum w(F_0^2)^2.$$

T a b l e 2

*Selected bond lengths (Å) and bond angles (deg.)*

Bond	Dist.	Angle	deg.	Angle	deg.
Fe(1)—N(1)	2.100(6)	Fe(1)—O(1)—Fe(1) #1	180.000(1)	N(1)—Fe(1)—N(2)	87.7(2)
Fe(1)—N(2)	2.084(6)	O(1)—Fe(1)—N(1)	106.76(18)	N(3)—Fe(1)—N(4)	85.7(2)
Fe(1)—N(3)	2.098(6)	O(1)—Fe(1)—N(2)	99.53(18)	N(2)—Fe(1)—N(4)	149.9(3)
Fe(1)—N(4)	2.112(6)	O(1)—Fe(1)—N(3)	101.69(19)	N(1)—Fe(1)—N(3)	151.4(3)
Fe(1)—O(1)	1.7739(12)	O(1)—Fe(1)—N(4)	110.59(19)	N(2)—Fe(1)—N(3)	87.1(2)

Symmetry transformations used to generate equivalent atoms: #1  $-x, -y+1, -z+1$ .

Table 3

Crystallographic structural parameters for three crystalline forms of [(OEPFe)<sub>2</sub>O]]

	Triclinic	Triclinic <sup>a</sup>	Monoclinic <sup>a</sup>
Space group	$P\bar{1}$ (#2)	$P\bar{1}$ (#2)	$P2_1/c$
$a, b, c, \text{\AA}$	10.915(4), 12.951(4), 13.403(4)	11.561(5), 12.299(8), 23.341(16)	18.433(13), 15.104(6), 23.489(6)
$\alpha, \beta, \gamma, \text{deg.}$	118.06(1), 100.33(1), 102.43(1)	82.56(3), 81.94(7), 79.18(1)	90.00, 97.82(1), 90.00
$V, \text{\AA}^3$	1144.5(1)	3210(5)	6479(9)
$Z$	1	2	4
Fe—O—Fe (deg.)	180.0	172.2	176.2
ave Fe—N ( $\text{\AA}$ )	2.096	2.077	2.080
Fe—O ( $\text{\AA}$ )	1.774	1.756	1.755
ave $\Delta^b$ ( $\text{\AA}$ )	0.53	0.50	0.54
ave sepn. <sup>c</sup> ( $\text{\AA}$ )	4.6	4.5	4.6
tilt <sup>d</sup> (deg.)	0.0	7.3	2.7
ave N—Fe—Fe—N (deg.)	1.2	17.0	16.8

<sup>a</sup> Data from [9].<sup>b</sup> The average displacement of the metal centers from the 24-atom cores.<sup>c</sup> The average mean plane separation for the two porphyrin cores of the dimer.<sup>d</sup> The interplanar angle between the two mean planes of the porphyrin dimer.

forms of  $\mu$ -O[Fe<sup>III</sup>(OEP)]<sub>2</sub> [9]. Also, the Fe—O bond distance is significantly shorter than those of any ( $\mu$ -hydroxo)diiron(III) complexes, whose values range from 1.96  $\text{\AA}$  to 2.06  $\text{\AA}$  [12].

The eight Fe—N bond distances have average values of 2.096  $\text{\AA}$ . The average Fe—N distance in [(OEPFe)<sub>2</sub>O] (1) is close to the 2.060—2.087  $\text{\AA}$  range expected for similar porphyrin complexes of the high-spin five-coordinate class [13]. The averaged Fe—N distance of [(OEPFe)<sub>2</sub>O] (1) is slightly longer than 2.077  $\text{\AA}$  and 2.080  $\text{\AA}$  in two forms of  $\mu$ -O[Fe<sup>III</sup>(OEP)]<sub>2</sub> and 2.037  $\text{\AA}$  of  $\mu$ -OH[Fe<sup>III</sup>(OEP)]<sub>2</sub>.

The average displacement of the metal centers from the 24-atom cores ( $\Delta = 0.53 \text{\AA}$ ) is longer than 0.50  $\text{\AA}$  in the triclinic form of  $\mu$ -O[Fe<sup>III</sup>(OEP)]<sub>2</sub> and 0.44  $\text{\AA}$  in  $\mu$ -OH[Fe<sup>III</sup>(OEP)]<sub>2</sub>, but it is shorter than 0.54  $\text{\AA}$  in the monoclinic form of  $\mu$ -O[Fe<sup>III</sup>(OEP)]<sub>2</sub>.

The interplanar angles between the mean 24-atom planes of a molecule for [(OEPFe)<sub>2</sub>O]] (1) is 0.0°. The average mean plane separations are 4.46  $\text{\AA}$  and close to those observed for two reported forms of  $\mu$ -O[Fe<sup>III</sup>(OEP)]<sub>2</sub>. Differences are seen in the bending about the Fe—O—Fe bond in porphyrin complexes [14]. Thus in [(OEPFe)<sub>2</sub>O] (1), the Fe—O—Fe angle is 180°, while in triclinic  $\mu$ -O[Fe<sup>III</sup>(OEP)]<sub>2</sub>, the Fe—O—Fe angle is 172.16(17)° and in monoclinic  $\mu$ -O[Fe<sup>III</sup>(OEP)]<sub>2</sub>, the Fe—O—Fe angle is closer to linearity: 176.2(2)°. The Fe—O—Fe angle of 180° is larger than 146.2(2)° of  $\mu$ -OH[Fe<sup>III</sup>(OEP)]<sub>2</sub>.

As reported by Scheidt *et al.* [9], the most important structural feature of the molecule in the two crystal forms is the near-eclipsed intramolecular porphyrin ring orientation. The averaged value of N—Fe—Fe'—N' twist angles are 17.0° in the triclinic form and 16.8° in the monoclinic form. Here, the averaged value of N—Fe—Fe'—N' twist angles is 1.2°; this is outside the general range [9] and [(OEPFe)<sub>2</sub>O] (1) has almost exactly eclipsed configuration and two rings are parallel.

Relative (inward/outward) orientations of the ethyl groups can be seen in Fig. 1. Four ethyl groups on each porphyrin are directed outward of the molecule, and four ethyl groups on each porphyrin are directed inward to the molecule. The locations of these peripheral ethyl groups have been identified as important contributors to the relative orientations of the two porphyrins and the Fe—O—Fe

angles in this  $\mu$ -oxo dimer. There is a difference between the relative orientations of ethyl groups to that observed for the reported monoclinic crystalline form of  $\mu$ -O[Fe<sup>III</sup>(OEP)]<sub>2</sub>.

**Acknowledgements.** We thank the University of Sistan and Baluchestan (USB) for the financial support.

#### REFERENCES

1. Deng Y., Huang M.J. // Chem. Phys. – 2006. – **321**, N 1-2. – P. 133 – 139.
2. Ricciardi G., Rosa A., Baerends E.J., Van Gisbergen S.A.J. // J. Amer. Chem. Soc. – 2002. – **124**, N 41. – P. 12319 – 12334.
3. Simonneaux G., Hindre F., Plouzennec M.L. // Inorg. Chem. – 1989. – **28**, N 5. – P. 823 – 825.
4. Cheesman M.R., Walker F.A. // J. Amer. Chem. Soc. – 1996. – **118**, N 31. – P. 7373 – 7380.
5. Safo M.K., Gupta G.P., Walker F.A., Scheidt W.R. // J. Amer. Chem. Soc. – 1991. – **113**, N 15. – P. 5497 – 5510.
6. Walker F.A., Nasri H., Tyrk I.T., Mohanrao K., Watson C.T., Shokhirev N.V., Debrunner P.G., Scheidt W.R. // J. Amer. Chem. Soc. – 1996. – **118**, N 48. – P. 12109 – 12118.
7. Bertini I., Gray H.B., Lippard S.J., Valentine J.S. // Bioinorganic chemistry, University Science books, Mill Valley, California, Chapter 4, 1994, p. 201.
8. a) Khorasani-Motlagh M., Safari N., Noroozifar M., Saffari J., Biabani M., Rebouças J.S., Patrick B.O. // Inorg. Chem. – 2005. – **44**, N 22. – P. 7762 – 7769; b) Khorasani-Motlagh M., Safari N., Noroozifar M., Shahroosvand H., Parsaii Z., Patrick B.O. // Inorg. Chim. Acta. – 2007. – **360**, N 7. – P. 2331 – 2338; c) Khorasani-Motlagh M., Safari N., Khavasi H.R., Noroozifar M., Shahroosvand H., Biabani M. // J. Chem. Crystallogr. – 2007. – **37**, N 7. – P. 457 – 461.
9. Cheng B., Hobbs J.D., Debrunner P.G., Erlebacher J., Shelnutt J.A., Scheidt W.R. // Inorg. Chem. – 1995. – **34**, N 1. – P. 102 – 110.
10. Altomare A., Burla M.C., Camalli M., Cascarano G.L., Gaiacovazzo C., Guagliardi A., Moliterni A.G.G., Polidori G., Spanga R. // J. Appl. Cryst. – 1999. – **32**, N 1. – P. 115 – 119.
11. Beurskens P.T., Admiraal G., Beurskens G., Bosman W.P., Gelder R., Israel R., Smits J.M.M. The DIRDIF94 Program System, Technical Report of Crystallography Laboratory, University of Nijmegen, The Netherlands, 1994.
12. Scheidt W.R., Cheng B., Safo M.K., Cukiernik F., Marchon J-C., Debrunner P.G. // J. Amer. Chem. Soc. – 1992. – **114**, N 11. – P. 4420 – 4421.
13. Scheidt W.R., Reed C.A. // Chem. Rev. – 1981. – **81**, N 6. – P. 543 – 555.
14. Lee H.M., Olmstead M.M., Gross G.G., Balch A.L. // Crystal Growth & Design. – 2003. – **3**, N 5. – P. 691 – 697.